EUROPEAN COOPERATION
IN THE FIELD OF SCIENTIFIC
AND TECHNICAL RESEARCH

EURO-COST

COST 259 TD(99) .....
Leidschendam,
The Netherlands
23-24 September 1999

SOURCE:
Technische Universität Wien
Institut füer Nachrichtentechnik und Hochfrequenztechnik

Helsinki University of Technology
Institut of Radio Communications

DIRECTIONAL WIDEBAND 3-D MEASUREMENTS OF MOBILE RADIO CHANNEL IN URBAN ENVIRONMENT

Juha Laurila, Klaus Hugl, Martin Toeltsch, Ernst Bonek
Technische Universität Wien,
Institut für Nachrichtentechnik und Hochfrequenztechnik
Gußhausstrasse 25/389, A-1040 Wien, AUSTRIA
Tel. +43-1-58801 38985, Fax. +43-1-58801 38999
Email. juha.laurila@nt.tuwien.ac.at

Kimmo Kalliola, Pertti Vainikainen
Helsinki University of Technology,
Institut of Radio Communications / Radio Laboratory
P.O. Box 3000, FIN-02015 HUT, FINLAND

DIRECTIONAL WIDEBAND 3-D MEASUREMENTS OF MOBILE RADIO CHANNEL IN URBAN ENVIRONMENT

Juha Laurila, Klaus Hugl, Martin Toeltsch, Ernst Bonek

Technische Universität Wien,
Institut für Nachrichtentechnik und Hochfrequenztechnik

Kimmo Kalliola, Pertti Vainikainen

Helsinki University of Technology,
Institut of Radio Communications

1 ABSTRACT

This paper describes novel 3-D radio channel measurements at the base station site in the urban environment. We introduce a new measurement concept which combines RF switching and synthetic aperture techniques and allows full 3-D characterisation of the channel. Additionally used dual-polarised patch antennas allow investigations both with vertical and horizontal polarisations. For estimation of the azimuth- and elevation angles of the incoming waves, we use high-resolution 2-D Unitary ESPRIT algorithm. We describe measurements with about 50 different transmitter positions and two receiver array sites with different antenna heights. Our results show that the environment seen by the base station strongly defines the propagation mechanisms. We demonstrate street canyon dominated propagation also when receiver array is at the rooftop level. We also show that signal components propagated over the rooftop are often related to the reflections from the high-rising buildings in the surroundings.

2 INTRODUCTION

Utilisation of adaptive antennas together with second and third generation mobile communication systems has raised significantly interest during last years [1]. Their potential for capacity improvement should not be underestimated. Realistic spatial channel models are prerequisite for the performance evaluation of different adaptive antenna solutions and estimation of the obtained capacity gain. See introduction of different modelling approaches in [2]. Another overview article [3] includes also considerations of different measurement techniques and extensive literature list. Realistic models require channel measurements to prove their assumptions and allow appropriate parameter selection.

This paper describes a measurement campaign carried out during a COST 259 STM as a co-operation between Helsinki University of Technology (Institute of Radio Communications) and Technische Universität Wien (Institut für Nachrichtentechnik und Hochfrequenztechnik). We performed dual-polarised wideband channel measurements at the base station site in the urban environment by applying a novel technique which enables to resolve *both azimuth- and elevation angles* of the incoming waves. Using a wideband channel sounder with a delay resolution of 33 ns the *full 3-D characterisation* of the channel is possible. Our measurement scheme combines the *RF-multiplexing* over the physical array with a *synthetic aperture* technique which allows to construct the virtual planar array structure. Our physical array consisted of 16 dual-polarised patch elements and the total size of the collected synthetic aperture was 16×58 elements ($8\lambda \times 29\lambda$)

Wideband 3-D measurements have been performed previously at the mobile station site at street-level [4], [5], but not at the base station (BS) site. Additionally, we are able to characterise the channel using both vertical- and horizontal polarisation. The spatial measurements at the BS site are especially interesting because the directions of arrival (DOA) are more discrete from the BS point of view. Also the implementation of the base station arrays is easier and therefore the first operational adaptive antenna

systems will use multiple sensors only at the BS. In this measurement campaign we used two different receiver array sites in an urban environment (downtown Helsinki). The antenna heights and positions corresponded to urban macro- and microcell antenna installations of the operational networks. The first position was clearly below the rooftop level of the surrounding buildings (microcell, RX1) and the second was at the rooftop level (macrocell, RX2).

The main goal of this measurement campaign was to improve understanding of the urban propagation mechanisms, e.g. by clarifying the following questions:

- What kind of environmental conditions lead to the street-canyon dominated propagation?
- Does the strongest direction of arrival (DOA) dominate the azimuthal delay power spectrum (ADPS) at the base station? or
- Are far reflected components (e.g. from the high-rising buildings in the surroundings) typical in a relatively flat urban environment?
- Do the signal components which are diffracted over the rooftop play a significant role?
- What is the role of the BS antenna height to all of these propagation mechanisms?

A further goal is to utilise all this provided information for channel modelling purposes.

3 MEASUREMENT CONCEPT & EQUIPMENT

3.1 General

Several techniques have been proposed for spatial channel measurements in the literature. In principle such measurements require a multi-channel vector sounder which is able to receive signals in a coherent manner from all antenna elements of the array. The channel description functions (e.g. impulse responses), can then be calculated by using these signal samples from different sensors which allows further the spatial characterisation of the channel (e.g. resolving the directions of arrival, DOA). However, this multi-channel sounding approach is not practical because of cost and complexity reasons. This kind of technique has been used only with narrowband measurements, e.g. in the framework of the TSUNAMI II project [6] using an 8-element linear array.

The practically appropriate alternative is to connect the elements of the array via fast RF-switches to a single channel sounder. Thus, sounding is performed periodically from each sensor. This kind of *RF-multiplexing* technique is feasible because the switching delays are very short, in the order of some nanoseconds. Spatial measurements using a single receiver with multiplexing are reported e.g. in [7] and [8].

The *synthetic aperture* technique is also widely used in spatial channel measurements. The idea is to collect sounding periods from different spatial positions using a single receiving antenna. With the sounding period we mean intervals when the receiver samples the signal to be able to define impulse responses as post-processing. Arbitrary array geometries can be created by predefining array aperture grid and moving a single sensor between these grid points. Another possibility is to move the receiver antenna with a constant speed and collect sounding periods with fixed intervals. The synthetic aperture technique has been used for urban macrocell measurements at the BS site [9] and at the MS site [10]. A basic requirement for the technique is that the channel remains static during the data collection period over the whole aperture.

In this paper we used a novel sounding technique, *combining RF-multiplexing* of different elements of the physical array and *synthetic aperture technique*. Our measurement system consisted of the physical array, trolley with electrical motor and IRC wideband channel sounder based on the direct sampling technique [7].

3.2 Construction of Synthetic Array

The physical array consisted of 16 dual-polarised patch antennas and was installed with vertical orientation on a trolley. The elements of the physical array were constructed to a "ziczac"-shape (see Fig. 1). In both directions the spacing between the antenna elements was λ/2. This structure reduced the mutual coupling between the elements essentially because the inter-element distance had a minimum of $1/\sqrt{2}\,\lambda$ between the corners of the patches. The trolley moved with a constant speed of 0,3m/s over the metallic rails.

During the measurements we collected "snapshots" over the physical array at certain horizontal positions. Each "snapshot" corresponded to one column in the grid of the synthetic planar structure. We took the following snapshot when the trolley had moved to the next horizontal position of the grid (distance between snapshots λ/2) and continued until 58 snapshots in different horizontal positions were collected. Thus, the physical dimensions of the synthetic aperture were 8×29 wavelengths. Figure 1 introduces the basic concept of the measurement and Fig.2. shows the measurement equipment at the microcell site.

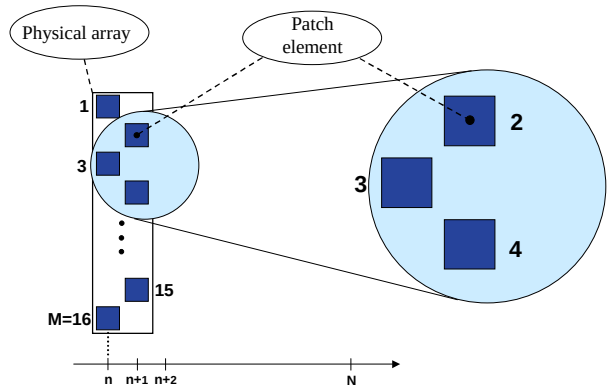

Fig.1. Measurement Concept

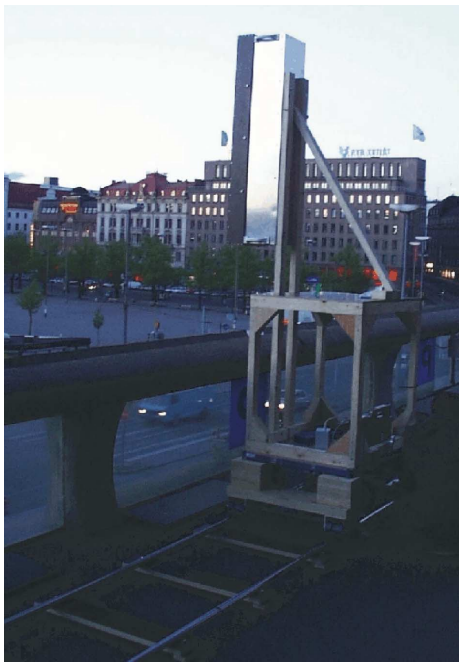

Fig. 2. Measurement System

3.3 Description of Used IRC Sounder

We utilised the wideband channel sounder developed at HUT/ IRC [11] using a carrier frequency of 2,154 GHz. The bandwidth of the system is 100 MHz. In these measurements we used the direct sampling mode of the equipment, which means that the I and Q branches of the received signal are sampled directly. The system provides impulse responses by correlating the used PN sequence and received signal samples (collected with oversampling rate 4) using software based post-processing. The chip frequency of the system is 30 MHz and thus the used PN-sequence with length of 255, leads to the maximum delay of 8,5μs with resolution of 33 ns. This delay range is adequate in the flat urban environment where the measurements were performed.

The used RF-multiplexer has a switching delay of 3ns. Thus, the snapshot collection period over the physical array was purely defined by the chip frequency and the used code length. In these measurements the data collection from all of the 16 dual-polarised elements lasted 544 μs. It is clear that uncertainty due to the constant movement of the trolley is negligible (the trolley moves during a snapshot collection period only $1{,}6 \cdot 10^{-4}$m).

4 HIGH-RESOLUTION DOA-ESTIMATION USING 2-D UNITARY-ESPRIT

After calculating the impulse responses of all synthetic sensor positions we reorganised the data so that the post-processing could be performed for a normal planar structure. The angular response was resolved from spatially varying impulse responses by using 2-D Unitary ESPRIT [12]. More thorough description of the data evaluation method can be found in [10] and [4] and in this paper we summarise only the basic principle.

From the impulse response averaged over all synthetic aperture elements, we selected all delay samples with power above the threshold value. Depending on the transmitter position and therefore on the SNR this dynamic range between the strongest peak of the impulse response and the selected threshold value varied between 15-30dB, but most values were above 25 dB. For each selected time instant we estimated L DOAs using the subspace estimation based 2-D Unitary ESPRIT algorithm [12] and 2-D spatial smoothing [13]. The optimal value for the number of DOAs, L_{opt}, was selected by minimising the so-called data estimation error, *DEE*, when the array steering matrix with different L values was used. After estimating these DOAs we created the corresponding array steering matrix and performed beamforming to be able to estimate the corresponding power. As an output we finally obtained DOAs (azimuth and elevation) and powers of L_{opt} incoming waves.

5 VALIDITY OF THE MEASUREMENT CONCEPT

The basic requirement for synthetic aperture measurements is that the channel is non-variant during the whole data collection period. Therefore, the measurements were performed during the night when the traffic in the surroundings was minimal. The snapshots in the different horizontal positions of the array were taken with the intervals of 0,24 s, which lead to the total data collection period of 14,5 s. Note, that this period is short compared to the case when one single antenna is moved manually over the grid points of the synthetic aperture. Thus, our technique does not set so strict requirements for the time-invariance of the channel. Note also, that the possible moving objects which might cause reflections are not in the vicinity of the array in the base station measurements, which further diminishes the static channel requirement.

The transmitter and receiver use rubidium standards with long time phase stability of $2 \cdot 10^{-11}$ as a frequency reference. The synchronisation was checked before and with constant periods also during the measurement session using the LOS (line of sight) scenario. This guaranteed the phase stability of the transmitter and receiver in all measurement positions.

We used LOS measurements also to validate the accuracy of the concept when the transmitter position was exactly known. By comparing the estimated azimuth and elevation angles to the geometrically calculated values we were able to secure the proper operation of the system during the whole measurement session. The estimated LOS values corresponded the real values with the estimation error smaller than 2°. Note, that this value includes also inaccuracies related to the positioning of the transmitter and the misalignment of the array. Additionally, plotting the phase variation of the LOS components over the whole synthetic array allowed to check the calibration of the system and stability of the trolley velocity.

We also eliminated the effect of the non-omnidirectional pattern of the individual antenna elements after the DOA estimation step. We multiplied the estimated power of incoming paths by the inverse of the measured antenna pattern with corresponding angle.

6 MEASUREMENT ENVIRONMENT

We carried out the measurements in an urban environment in downtown Helsinki (in the vicinity of the central railway station). We used two receiver array sites, RX1 on the second floor level below the rooftop and RX2 at the rooftop level. These receiver positions correspond well to the real micro- and macrocell antenna installations in urban environments. Figure 3 shows the map of the area including the selected sample transmitter positions.

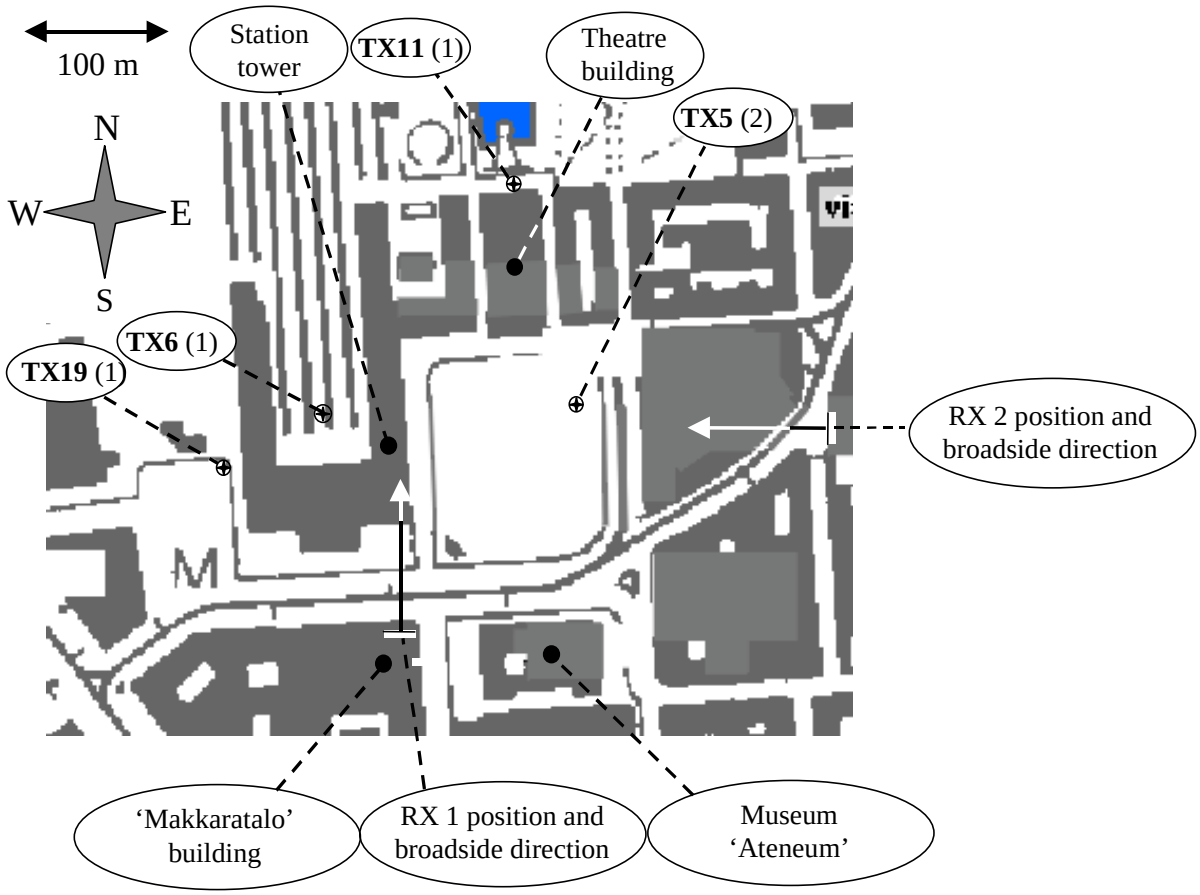

Fig. 3. Overview map with selected TX positions

At the RX1 site the environment is more open compared to the other site. In front of the array there is the railway station with an open and flat railway yard behind it. The open square (Rautatientori) dominates the environment to the right of the antenna broadside (see Fig.4). Behind the first block on the northern side of the square there is a park. This means that far reflections from the north (broadside direction of the array) are not possible. The main entrance of the railway station with large windows was on the street level about -40° left from the antenna broadside. The station tower directly in front of the array is also worth mentioning. Most transmitter positions were collected in the narrow street-canyons or on the railway yard behind the station building.

The characteristic environmental feature for the second receiver position (RX2) was the broad street ('Kaisaniemenkatu') approaching the receiver from left with the angle of about -25° from the broadside (see Fig. 5). The open square in the vicinity allowed coupling of the energy to this broad street in most cases. The height of building blocks beside and in front of the array is equal to antenna height. Only the tower of the theatre building on the northern side of the open square rises slightly above the other environment (see Fig.4). However, there was no direct line-of-sight (LOS) between tower and receiver array. Transmitter positions were collected on the square and in the different types of street canyons leading to the different physical propagation conditions.

Figure 4 shows the view from the RX1 (microcell) site towards the open square and Fig. 5 from the RX2 site (macrocell) towards the street.

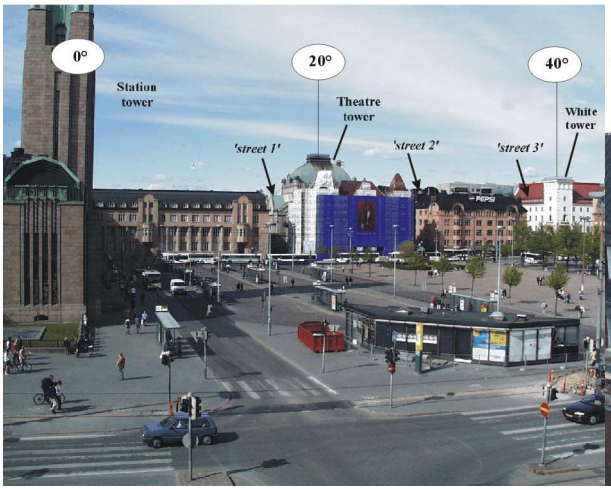

Fig. 4. View from RX1 site (microcell)

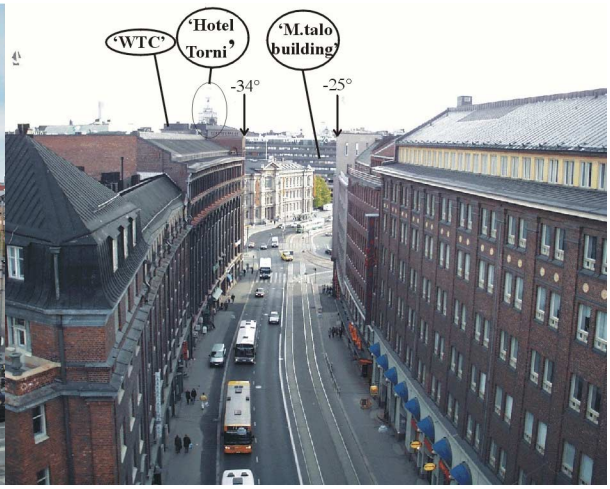

Fig. 5. View from RX2 site (macrocell)

The delay spread, DS, values obtained in our measurements correspond well with the typical urban values shown in literature. For the RX1 (RX2) site mean DS value was 1,27 μs (1,19 μs) and the values varied between 0,69-2,32 μs (0,53-2,37 μs), respectively.

7 RESULTS

During the measurement campaign we collected data using about 50 different transmitter positions. In this paper we only show some sample results. These selected examples show the most typical propagation mechanisms observed in the measurements. Thus, these samples support the conclusions drawn in the subsequent chapter, even if they are drawn using the whole measurement set available. With these examples we can already demonstrate several different propagation mechanisms.

To make the interpretation of the results easier, we collect the incoming waves to clusters according to the physical propagation routes and these classes are also shown in the detailed maps describing each measurement position. The names of the clusters are shown in *italic* in the text.

We show results for the both measured polarisations. The notation Pol.2. means that the transmitter and receiver antenna have the same polarisation and in case of cross-polarisation notation Pol.1. is used. In the cross-polarised case we received on average 7 dB less power. However, we discuss some transmitter positions in detail only from cross-polarisation point of view because in some cases it showed more interesting propagation mechanisms.

7.1 RX1 - Array below the Rooftop Level (Microcell)

7.1.1 Transmitter position TX11 (1)

Transmitter position 11 situates on the street behind the building block on the northern side of the 'Rautatientori' square. This position shows different behaviour with different polarisations and we consider both of them separately below. When the same polarisation (Pol.2) is transmitted and received the narrow street canyons on both sides of the theatre building (Fig.4, Fig.6) fully define the propagation scenario. All waves arrive with low elevation angles from the azimuthal directions defined by parallel streets (*'street1 - street3'*). The western street (*'street 1'*) dominates but some waves with short delays arrive also from *'street 3'*. However, we observe also components with relatively long delays which correspond to

reflections from the park (north from the transmitter) and multiple reflections in the street canyons. Figure 6 shows a detailed map of the surroundings of the transmitter and Fig.7 and Fig.8 azimuth-elevation and delay-azimuth planes, respectively.

Considering cross polarisation the situation is different. The signal components from the first and second street exist still but the coupling to the *'street 3'* does not play a role any more. As a significant difference to the previous case we now observe also strong diffracted components with high elevation angles from the tower of the theatre (*'theatre tower'*). Spreading in the delay domain is also somewhat shorter. Figure 9 demonstrates the difference between polarisations using an azimuth-elevation plot.

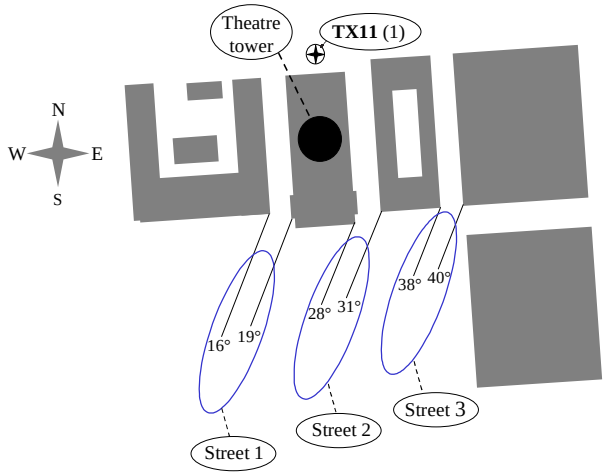

Fig.6. TX 11: Detailed map

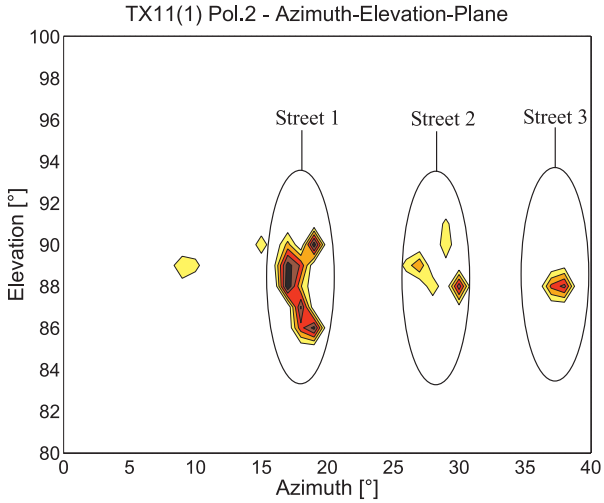

Fig.7. TX 11: Azimuth-elevation plane, same-pol.

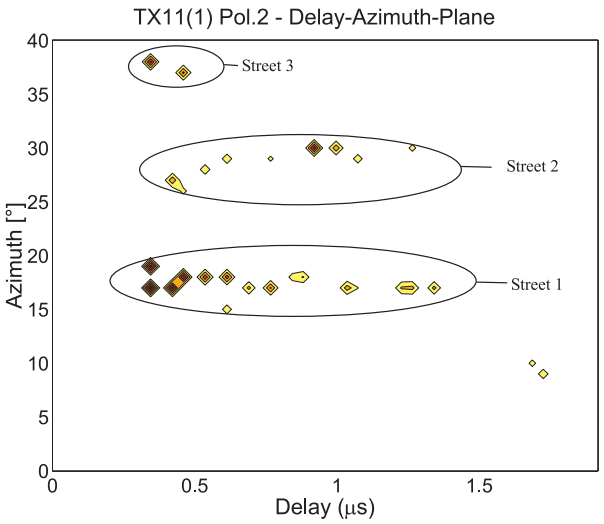

Fig.8. TX11: Delay-azimuth plane, same-pol.

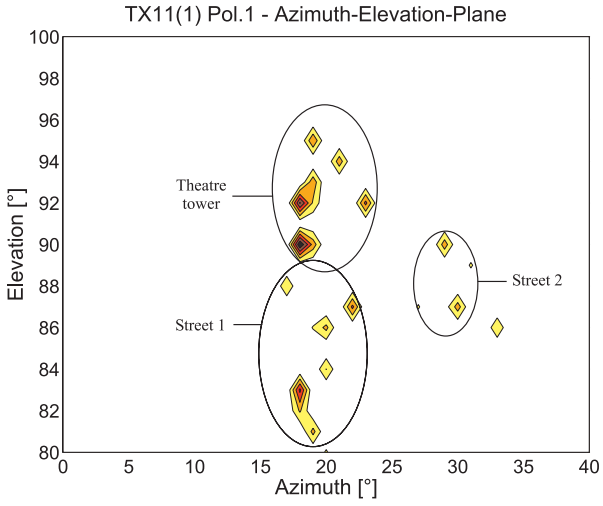

Fig.9. TX11: Azimuth-elevation plane, cross pol.

7.1.2 Transmitter position TX19 (1)

The transmitter position TX19 is on the western side of the railway station. With our 3D analysis we can separate several different propagation mechanisms related to this position. For this position we show results only for cross-polarised case. The earliest components in the delay domain arrive as a diffraction around the left corner of the station (*'around corner'*). We can also observe significantly delayed components from this direction which are reflected from the 'post building' (Fig.10) (*'post'*). These waves also show somewhat higher elevation angles than the components originated from diffraction. The second

visible component is reflection from the tower of the railway station in the broadside direction. This component (*'station tower'*) shows a very high elevation angle. The waves related to the next cluster arrive approximately from the direction of the pseudo-LOS and they show high elevation angles. With the pseudo-LOS we mean the direction of the line connecting the MS and BS compared to the antenna broadside. These components are diffracted over the roof of the station (*'over roof'*). They also show spreading in delay which signifies that some of them have experienced reflections from the post building and other objects before diffraction over the rooftop. The next observed cluster is related to multiple reflections in the street canyon below the receiver array. The elevation angles of these waves differ significantly. Some of them arrive from the street level whereas others have reflected from the wall of the station building ('*street reflections*'). The last components in the delay domain arrive from the direction of the square. Their origin seems to be reflection from the small building situated in the south-western corner of the square. Figure 10 shows a detailed map including angular information, and Figs.11 and Fig.12 demonstrate the azimuth-elevation and delay-azimuth behaviour for the cross-polarised case, respectively.

With the same polarisation transmitted and received the situation is essentially simpler. In that case '*around corner'* and '*over roof* ' propagation fully dominates the situation.

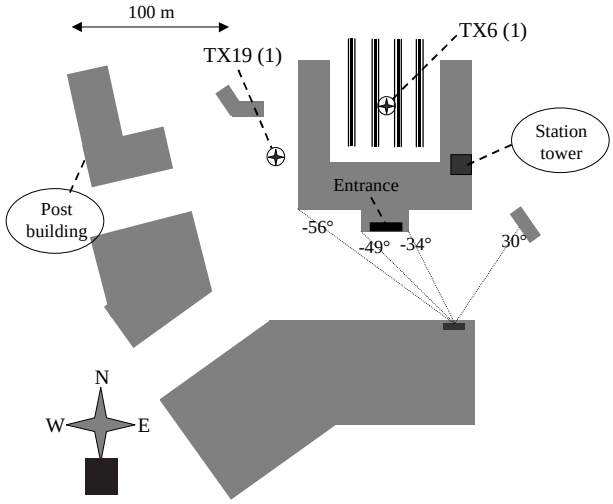

Fig.10. TX19/TX6: Detailed map

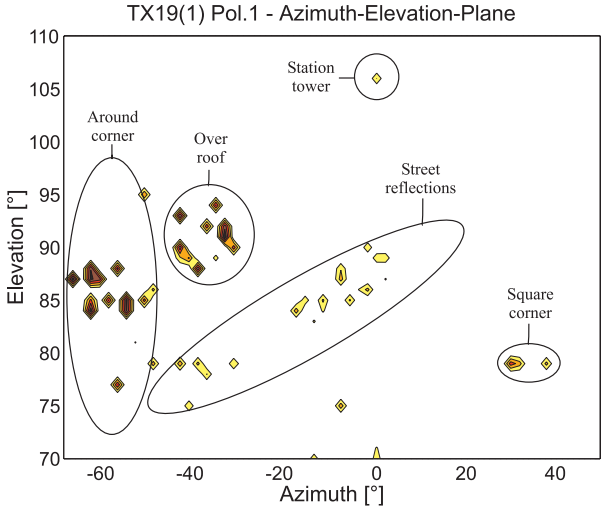

Fig.11. TX19: Azimuth-elevation plane, cross-pol.

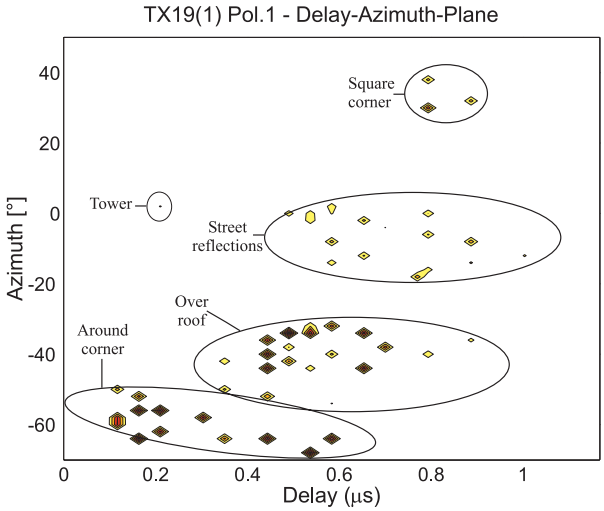

Fig.12. TX19: Delay-azimuth plane, cross-pol.

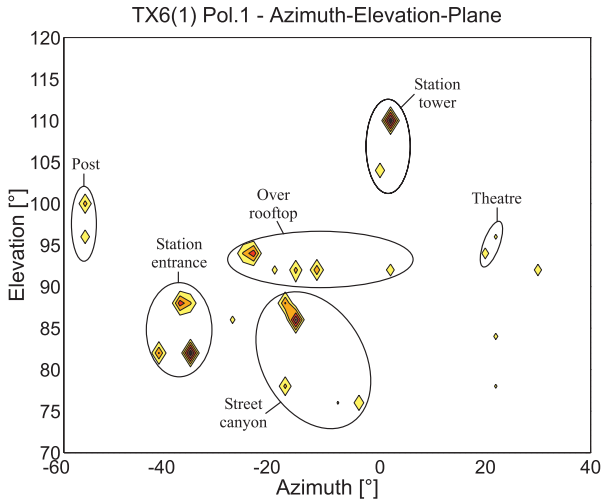

Fig.13. TX6: Azimuth-elevation plane, cross-pol.

7.1.3 Transmitter position TX6 (1)

The transmitter position TX 6 situates on the railway yard near the entrance of the station building. The main entrance of the station with large windows is on the opposite side of the building and these two entrances are connected with a relatively open corridor. We start considerations with the cross-polarised case. In the delay domain the first components arrive through the building and at the receiver site they are seen with a low elevation angle and azimuthal angle of about -40° (*'station entrance'*). These components show short spreading in the delay domain. The propagation over the roof begins almost simultaneously (*'over rooftop'*). The first components are originated by direct diffraction but due to the reflections from the objects in the railway yard also more delayed waves exist. In addition to the diffraction over the roof we also see a reflected component from the station tower (Fig.4, Fig.10). This component (*'tower'*) has a very high elevation and it carries strong power in this scenario. From the tower direction we also see some delayed components which are results of multiple reflections. In the street canyon below the receiver array ('Kaivokatu') a lot of different reflectors exist. We also observe delayed components with low elevation angles in the azimuthal range between 0° and -20° which are related to multiple reflections from these objects and the wall of the station building (*'street canyon'*). It might be also possible that some of these waves experience multiple reflections inside the station and impinge to the receiver through the windows of the building. The last arriving signal components are related to far reflections from the post building on the left hand side (*'post'*) and the tower of the theatre on the northern side of the square (*'theatre'*) (see Figs.4 and Fig.10). Figures 14 and 15 show the received power over azimuth-elevation and delay-elevation planes, respectively.

With the same polarisation the main difference is related to the existence of the reflected components. The reflection from the tower which carries the same power as the propagation via the entrance in the cross-polarised case does not exist any more. Thus, in this case the role of *'over rooftop'* propagation is more significant. Also the reflections from the tower of the theatre building are not present. Figures 16 and 17 demonstrate the difference between polarisations by azimuth-elevation and delay elevation plots.

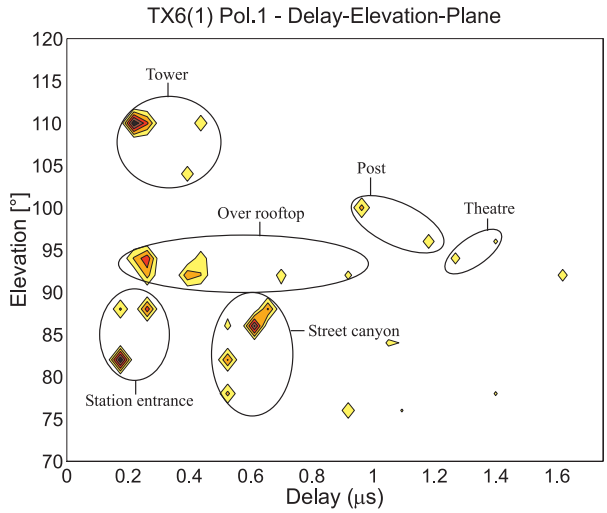

Fig.14. TX6: Delay-elevation plane, cross-pol.

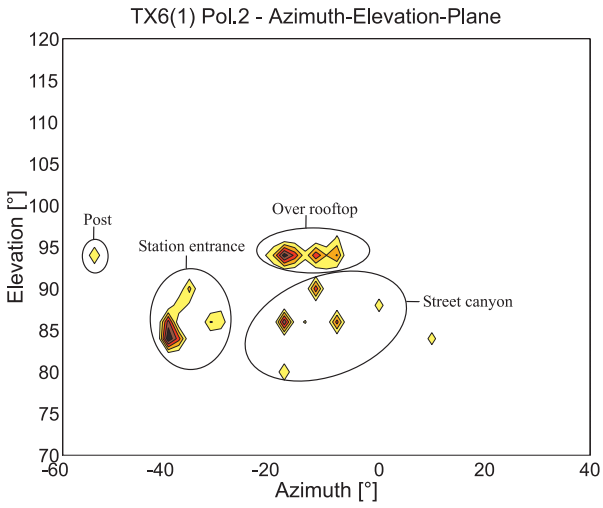

Fig.15. TX6: Azimuth-elevation plane, same pol.

7.2 RX2 - Array at the Rooftop Level (Macrocell)

7.2.1 Transmitter position TX5 (2)

The transmitter position TX5 (2) is situated near the north-eastern corner of the open square. For this position we discuss the cross-polarised case more in detail. The first signal component arrives from the pseudo-LOS direction diffracted over the rooftop (*'pseudo-LOS'*). Only slightly delayed waves arrive from the azimuth angle of about 30° which corresponds to the reflections from the white relatively high-rising building in the corner of the square (*'white tower'*) (Fig. 4 and Fig.17). Simultaneously with these

reflections also the first components from the direction of the 'Kaisaniemenkatu' (*'street canyon'*) begin to arrive. From this direction we see spreading in the delay domain because all reflected components from the 'Makkaratalo building' and 'Museum Ateneum' arrive from this azimuthal range. Note also, that these street canyon propagated waves have dependence between elevation and delay. The signal components arriving with the shortest delays are diffractions from the corners of the street canyon and they show the lowest elevation angles. Also the elevation angle increases as a function of delay (see Fig. 20). Some of the street canyon propagated components experience local scattering effects near the base station and they show low elevation angles (*'street canyon scattering'*). Slightly after the first street canyon diffracted components we observe reflections from the tower of the theatre (*'theatre'*) building on the northern side of the square (Fig. 4 and Fig.17).

Figures 18-20 show azimuth-elevation, delay-azimuth and delay-elevation planes for the cross-polarised case, respectively.

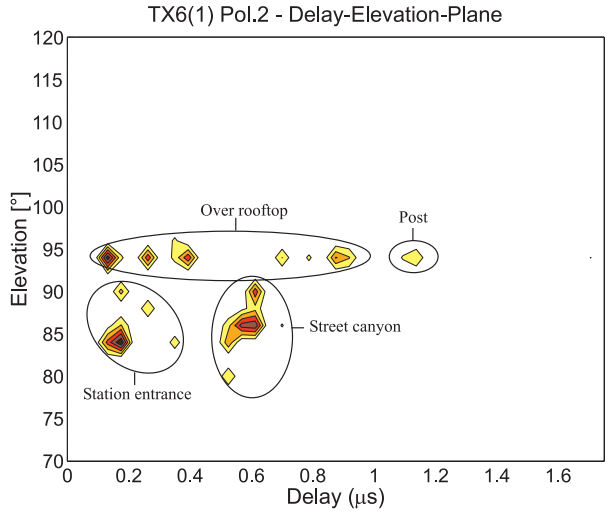

Fig.16. TX6: Delay-elevation plane, same pol.

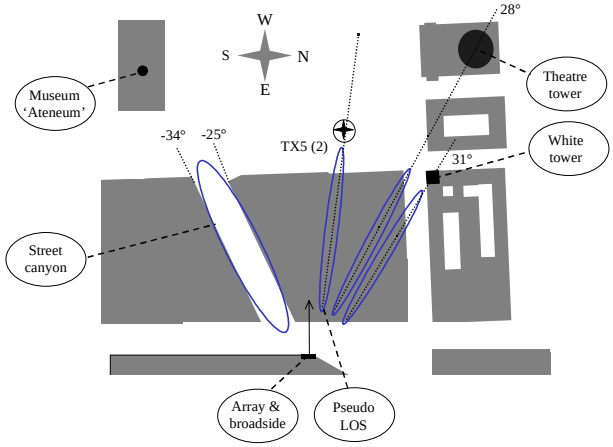

Fig.17. TX5: Detailed map

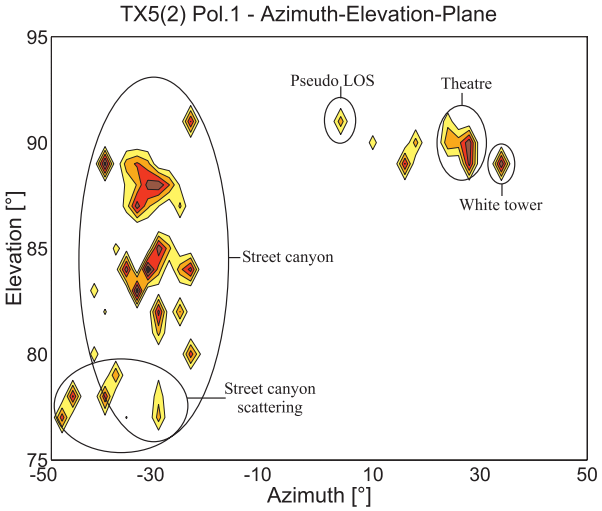

Fig.18. TX5: Azimuth-elevation plane, cross-pol.

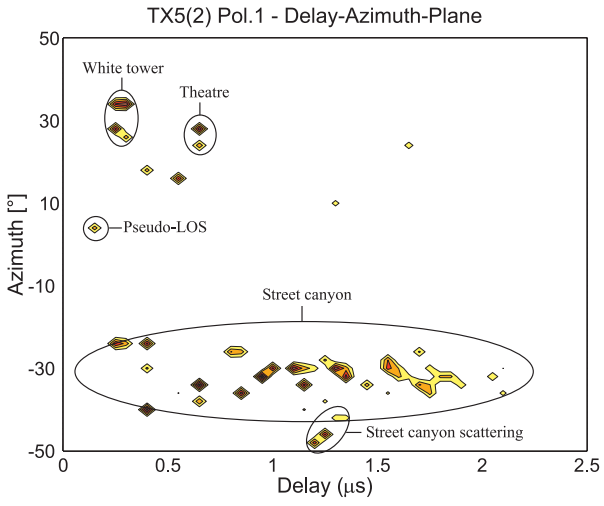

Fig.19. TX5: Delay-azimuth plane, cross-pol.

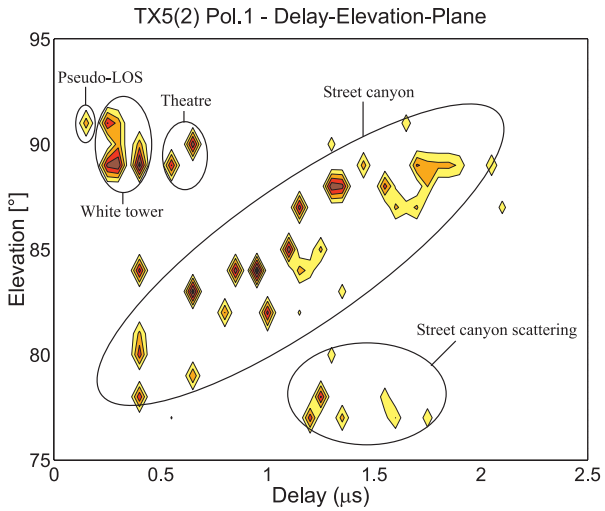

Fig.20. TX5: Delay-elevation plane, cross-pol.

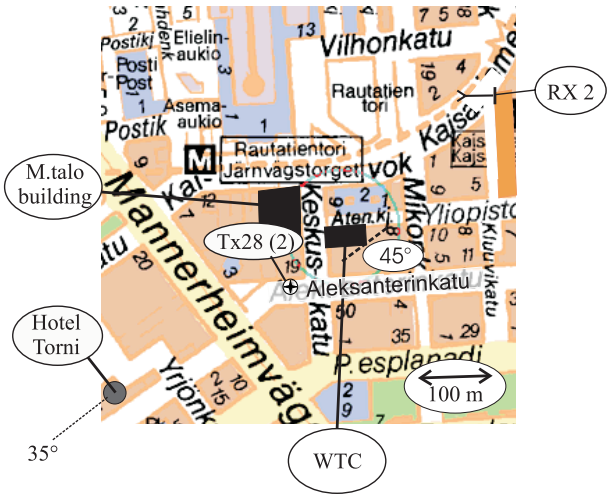

Fig.21. TX28: Detailed map

7.2.2 Transmitter position TX28 (2)

On the contrary to the other selected sample results this position does not show a typical behaviour, but due to the interesting effect observed it is worth mentioning. Also with this position we mainly consider cross-polarisation. In this case transmitter position was in the street canyon of 'Aleksanterinkatu'. From the transmitter there is a LOS connection to the highest building in the surroundings (*'Hotel Torni'*) rising clearly above the other ones. The top of this building also has a LOS connection to the RX site (see Fig.5). The reflected component from 'Hotel Torni' arrives about 1,5 µs after the first components and has the strongest power. For the first arriving waves two different propagation mechanisms exist. One component propagates over the rooftop with the azimuth angle of -45°. The relatively high-rising 'World Trade Center, WTC' building (see Fig.5 and Fig.21) seems to block all components in the azimuthal range between -35° and -45° and this wave is probably originated as a diffraction from the left corner of the WTC building (*'WTC'*). Another significant short delay component is related to the coupling of the signal energy to the street canyon of 'Keskuskatu' and the signal is observed at the receiver after reflections from the 'Makkaratalo' building.

Figure 21 shows the map including the transmitter position and assumed dominating propagation paths. Figures 22-24 show the power delay profile, azimuth-elevation and delay-azimuth planes, respectively, in the cross-polarised case.

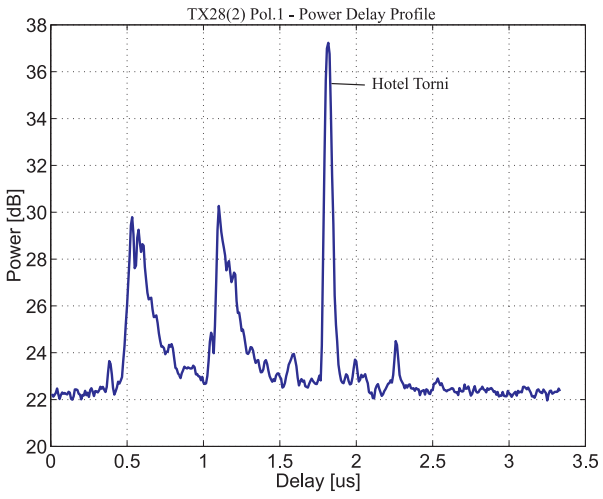

Fig.22. TX28: Power delay profile, cross-pol.

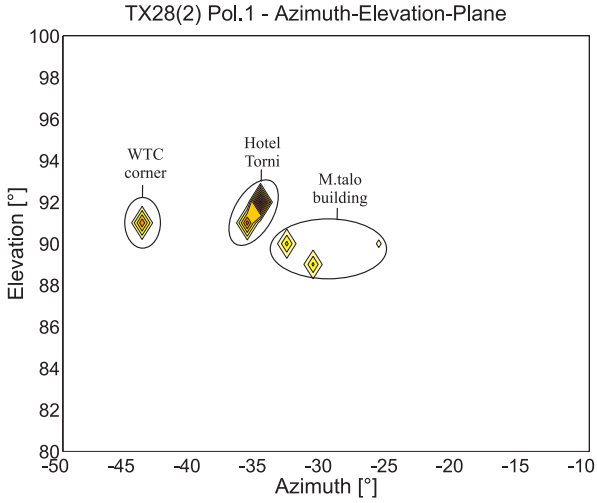

Fig.23. TX28: Azimuth-elevation plane, cross-pol.

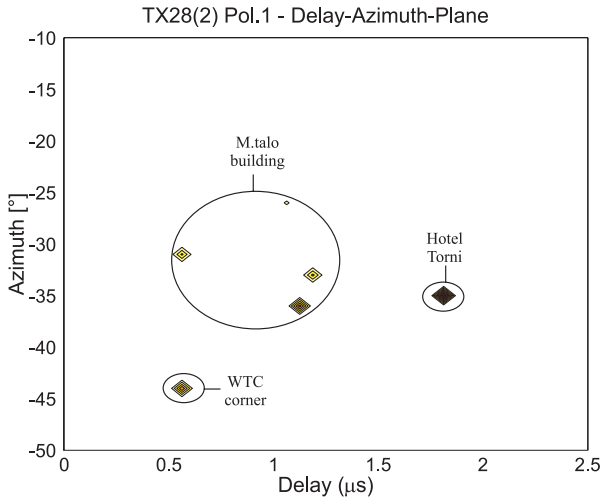

Fig.24. TX28: Delay-azimuth plane, cross-pol.

As a summary of the second receiver array position we conclude that independently of the transmitter position almost always the same propagation mechanisms were present. In the angular domain, we always observed strong signal components from the direction of the street ('Kaisaniemenkatu') and often the reflections from the tower of the theatre building. Thus, the sample position TX5 shows a very typical behaviour. The only feature which varied depending on the transmitter position was the relative delay between these dominating propagation mechanisms.

8 CONCLUSIONS

The analysis of the results lead to the following conclusions. We have drawn these conclusions after evaluating the whole measurement set, not only from the examples shown in this paper.

- The propagation scenario is strongly defined by the environment seen by the BS. For example, with RX2 site (macrocell) the main part of the energy was always received from the direction of the street canyon independently of the position of the mobile station. Note, however that the open square might make this kind of 'canyoning' behaviour stronger because it allowed coupling of the energy to the street canyon of 'Kaisaniemenkatu' in most transmitter positions. Thus, this kind of effect might be weaker in pure 'Manhattan grid' environment.

- The environment seen from the receiving array plays a more significant role for the propagation mechanisms than the RX antenna height. As already mentioned, the street canyon propagation dominated and the 'over the rooftop' components were weak in case of RX2 site, even through it was situated at the rooftop level. With the lower antenna height (RX1) a more significant 'over the rooftop' propagation was present. Thus the behaviour seen in these measurements was contrary to the common assumption that diffraction over the rooftop becomes more significant with higher antenna installations. Of course, the role of antenna height can be clarified only by performing measurements exactly at the same location with array installations over and below rooftop level. Especially with this kind of synthetic aperture measurements which require quite a lot space at the receiver site, it is difficult to find suitable receiver positions allowing that. However, from these measurements we can conclude that definitely the antenna height is not the only factor defining signal characteristics at the base station.

- The propagation over the rooftops is typically related to the far reflections. Note, that this happened also in our relatively flat environment where really high-rising buildings did not exist. Directly diffracted components arriving with the shortest delays from the geometrical direction of the transmitter (pseudo-LOS) were always weak and in many cases they did not exist at all. The tower of the railway station and the theatre building acted as typical reflectors corresponding to RX1 and RX2 sites, respectively.

- The local scattering effect in the surroundings of the MS does not typically play a significant role if we consider the situation from the base station point of view. The signal components arriving from the direction of the pseudo-LOS were normally weak and showed short spreading in the delay domain. Also the local scattering in the vicinity of the BS did not play an essential role in these measurements even if the base station site (RX1) was located below the rooftop level. On the street level below the base station a lot of possible reflectors were present, but only some reflections from them were observed. Note, however, that the environment seen from this site was quite open which reduces the effect of the local scattering. In general, when the base station is in the narrower street canyon without any open areas in the vicinity, the local scattering effect will be stronger.

- The dependence between the environment seen by the base station and the propagation mechanisms seems to be to strong in this kind of typical urban environment. This means that accurate prediction of the signal strength and quality at the specific BS site seems to require accurate ray-tracing based simulation tools utilising a building database (including also the height information). This might be even more important when network planning is carried out for adaptive antenna base stations. The data set collected by our 3-D measurement would also allow efficient evaluation of existing ray tracing tools.

- If we consider these measurements from the adaptive antenna point of view, we can see that also the urban channel has a strong directional nature. In most of our measured cases we were able to identify dominating propagation paths and thus the adaptive antenna processing at the base station can provide expected gains. On the other hand, the spatial separation of the users, which is required in space division multiple access (SDMA) operation (more than one user per traffic channel), is difficult especially in environments corresponding to our second measurement site RX2.

Acknowledgements: Authors would like to thank for Mr. Martti Toikka and Mr. Viktor Nässi for their help during the measurement campaigns and colleagues of the INTHF/mobile communication group and IRC/radio laboratory for fruitful technical discussions. The measurements were carried out during the COST 259 short-term mission. This work was also partially made in the framework of the projects funded by Austrian Science Fund (P-12147-ÖMA) and Technology Development Centre, Finland (TEKES). Financial support of the Academy of Finland, Wihuri Foundation and Emil Aaltonen Foundation is also gratefully acknowledged.

REFERENCES

[1] A.J. Paulraj, C.B. Papadias, Space-Time Processing for Wireless Communications, IEEE Signal Processing Magazine, Vol.14, No.5, Nov.1997, pp. 49-83.

[2] R.B. Ertel, P. Cardieri, K.W. Sowerby, T.S. Rappaport, J.H. Reed, Overview of Spatial Channel Models for Antenna Array Communications Systems, IEEE Pers. Comm., Vol.5. No.1, Feb. 1998, pp. 10-22.

[3] U. Martin, J. Fuhl, I. Gaspard, M. Haardt, A. Kuchar, C. Math, A.F. Molisch and R. Thomä, Model Scenarios for Intelligent Antennas in Cellular Mobile Communication Systems - Scanning the Literature. Wireless Personal Communications Magazine 11, Special Issue on Space Division Multiple Access, p. 109-129, 1999

[4] A. Kuchar, J-P Rossi and E. Bonek, Directional Macro-Cell Channel Characterization from Urban Measurements, IEEE Trans. on Antennas and Propagation, *accepted for publication*

[5] K. Kalliola, H. Laitinen, Statistical Distribution of Incident Waves to Mobile Antenna in Microcellular Environment at 2.15 GHz, COST 259 Meeting, TD(99)45,Vienna, Austria, April 20-21, 1999

[6] P. Mogensen, *et.al.*, Preliminary measurement results from an adaptive antenna array testbed for GSM/UMTS. IEEE Vehicular Technology Conference (VTC '97), Phoenix, AZ, May 1997.

[7] K. Kalliola and P. Vainikainen, Characterization System for Radio Channel of Adaptive Array Antennas, IEEE Conf. Proc. PIMRC '97, Helsinki, Sep. 1997, p. 95-99.

[8] U. Trautwein, K. Blau, D. Brückner, F. Herrmann, A. Richter, G. Sommerkorn, R. Thomä, Radio Channel Measurement for Realistic Simulation of Adaptive Antenna Arrays. 2nd European Personal Mobile Communications Conference EPMCC '97 /, Bonn, September 1997, p. 491-498.

[9] U. Martin, Spatio-Temporal Radio Channel Characteristicsin Urban Macrocells, IEE Proc. Radar, Sonar and Navigation, Vol. 145, No.1, February 1998, p. 42-49.

[10] J. Fuhl, J.-P. Rossi, and E. Bonek, High-Resolution 3-D Direction-of-Arrival Determination for Urban Mobile Radio, IEEE Tr. on Antennas and Propagation, Vol. 45., No.4, Apr. 1997, p. 672-682.

[11] J. Kivinen, T. Korhonen, P. Aikio, R. Gruber, P. Vainikainen, S.-G. Häggman, Wideband Radio Channel Measurement System at 2 GHz, IEEE Transactions on Instrumentation and Measurement, Feb. 1999, *in press*

[12] M.D. Zoltowski, M. Haardt and C.P. Mathews, Closed-Form 2-D Angle Estimation with Rectangular Arrays in Element Space of Beamspace via Unitary ESPRIT, IEEE Trans. on Signal Proc. Vol.44. No2. Feb. 1996, p. 316-328.

[13] T.-J. Shan, M. Wax and T. Kailath, On Spatial Smoothing for Direction-of-Arrival Estimation of Coherent Signals. IEEE Trans. on Acoustics, Speech and Signal Proc. Vol. 33, No.4., Aug. 1985, p. 806-811.